



Investigation of absorption and scattering characteristics of kiwifruit tissue using a single integrating sphere system*

Zhen-huan FANG, Xia-ping FU^{†‡}, Xue-ming HE

(College of Biosystems Engineering and Food Science, Zhejiang University, Hangzhou 310058, China)

[†]E-mail: fuxp@zju.edu.cn

Received Apr. 15, 2015; Revision accepted Nov. 30, 2015; Crosschecked May 11, 2016

Abstract: For a quantitative understanding of light interaction with fruit tissue, it is critical to obtain two fundamental parameters: the absorption coefficient and the scattering coefficient of the tissue. This study was to investigate the optical properties of kiwifruit tissue at the wavelength of 632.8 nm. The total reflectance and total transmittance of kiwifruit tissue from three parts (including the flesh part, the seed part, and the seed-base part) were measured using a single integrating sphere system. Based on the measured spectral signals, the absorption coefficient μ_a and the reduced scattering coefficient μ_s' of kiwifruit tissue were calculated using the inverse adding-doubling (IAD) method. Phantoms made from Intralipid 20% and India ink as well as a Biomimic solid phantom were used for system validation. The mean values of μ_a and μ_s' of different parts of the kiwifruit were 0.031–0.308 mm^{-1} and 0.120–0.946 mm^{-1} , respectively. The results showed significant differences among the μ_a and μ_s' of the three parts of the kiwifruit. The results of this study confirmed the importance of studying the optical properties for a quantitative understanding of light interaction with fruit tissue. Further investigation of fruit optical properties will be extended to a broader spectral region and different kinds of fruits.

Key words: Optical properties, Integrating sphere, Inverse adding-doubling, Kiwifruit
<http://dx.doi.org/10.1631/jzus.B1500086>

CLC number: S123

1 Introduction

Visible-near infrared (Vis-NIR) spectroscopy has been widely applied for nondestructive assessment of the physical and chemical quality parameters of fruits by many research groups as well as companies. In conventional Vis-NIR spectral analysis, the spectra are always described by the absorbance of light based on Beer-Lambert Law (or Beer's Law). The concentration of the compounds is proportional to the absorbance (Chen and Wang, 2001). Quality

assessments are typically executed based on large datasets using chemometrical methods. In this way, scattering is weakened or neglected, as well as are the complex light propagations inside the fruits. However, as a kind of turbid biological material, the constituents and structures of fruit tissue are very complex. Information about the interaction between light and fruit tissue is essential in the evaluation of fruit qualities, since optical signals are significantly affected by constituents and the physical structure of tissue. In light penetration in multiple scattering media, such as fruit, both scattering and absorption contribute to the distance-dependent attenuation. For a quantitative understanding of light interaction with fruit tissue, it is critical to obtain two fundamental optical properties characterized by the absorption coefficient (μ_a) and the scattering coefficient (μ_s) (Tuchin, 2007). The measured absorption and scattering coefficients can

[‡] Corresponding author

* Project supported by the National Natural Science Foundation of China (No. 31401289), the Zhejiang Provincial Natural Science Foundation of China (No. LQ12C10001), and the Education Department of Zhejiang Province (No. Y201122219), China

ORCID: Xia-ping FU, <http://orcid.org/0000-0002-4156-668X>

© Zhejiang University and Springer-Verlag Berlin Heidelberg 2016

be used not only for characterizing the absorption and scattering features, respectively, of fruit and vegetable tissues, but also for such investigations and applications as simulating light propagation inside tissues, assessing qualities of fruits and vegetables, and providing guides for their process optimization. Most studies measured the reduced scattering coefficient (μ_s') instead of μ_s . The relationship between μ_s' and μ_s is $\mu_s'=(1-g)\mu_s$, where g is the anisotropy factor.

In biomedical engineering research, different methods have been used to measure absorption and scattering properties of different types of biological tissue (Cheong *et al.*, 1990; Tuchin, 2007). More information about the tissue is obtained because absorption and scattering properties are distinguished. All these methods can be classified into direct and indirect methods according to the theory and technique based on the study of Kim and Wilson (2011). Because of the critical experimental conditions that direct methods need, most methods reported are indirect methods (Tuchin, 2007). Inverse adding-doubling (IAD) is one of the indirect methods based on adding-doubling theory. It usually uses an integrating sphere-based system to measure the transmittance and reflectance of the tissue. Then, the optical properties of the measured tissue can be calculated in the inverse form of adding-doubling (Pickering *et al.*, 1993; Prahl *et al.*, 1993; Prahl, 2011). Compared with other commonly used methods such as the time-resolved method, the spatially-resolved method, and the frequency-domain method, the integrating sphere method has the characteristics of low cost, being easy in execution, but slow speed. It is suitable for initial research on tissue optical properties. It is also a favorable method for comparison purposes to validate the measurement results of other methods because of the relatively accurate results that can be gained by this method.

Research on light transportation in agro-food products can be dated back to the report of Birth (1978), who studied the relationship between the light scattering properties and internal structure of raw plant and pork tissue with a high moisture content. They pointed out that the physical structure of agro-products determined its scattering and the composition determined its absorption. Little progress was made until the 21st century; an important reason for this may be that Vis-NIR spectroscopy attracted the attention of researchers because of its

fast speed and simple sample preparation advantages. In the past decade, investigations for measuring tissue absorption and scattering coefficients of agro-products became popular for the previously mentioned reasons. Much attention was paid to the optical properties of apples perhaps because of the universality of this crop (Cubeddu *et al.*, 2001a; 2001b; Zerbini *et al.*, 2002; Qin and Lu, 2008; 2009; Vanoli *et al.*, 2009; 2014; Lu *et al.*, 2010; Rizzolo *et al.*, 2010). Other fruits (peach (Cen *et al.*, 2012), pear (Zerbini *et al.*, 2002), plum (Qin and Lu, 2008), etc.) and vegetables (tomato (Cubeddu *et al.*, 2001a), cucumber (Qin and Lu, 2008), onion (Wang and Li, 2013), etc.) were also studied but not as frequently. In the studies by two groups, the method of time-resolved spectroscopy (TRS) was mostly used by the research group at CRA-IAA (Consiglio per la Ricerca e la Sperimentazione in Agricoltura, Unità di ricerca per i processi dell'industria agroalimentare) in Italy and the hyperspectral imaging-based spatially resolved (HISR) method was mostly used by the research group in ARS/USDA (Agricultural Research Service, United States Department of Agriculture) at East Lansing, Michigan, USA. Although rare, research about absorption and scattering properties of kiwifruit was carried out by the two groups (Zerbini *et al.*, 2002; Qin and Lu, 2008). There were some reports on optical property measurements of fruits and vegetables based on single integrating sphere: Saeys *et al.* (2008) used single integrating sphere measurements combined with IAD to estimate the optical properties of apple skin and flesh tissue in the 350–2200 nm range for three cultivars. Wang and Li (2012; 2013) measured the optical properties of skin and fleshy tissues of onion at 632.8 nm to better understand their light propagation. The results indicated that onion dry skins have much higher absorption and reduced scattering coefficients compared with onion fleshy tissues. They also found that, for both skin and flesh, the μ_a varied between cultivars, while the differences of the μ_s' between cultivars were less profound.

A preliminary work was presented at 2014 American Society of Agricultural and Biological Engineers (ASABE) Annual International Meeting (Fang and Fu, 2014). After that, the measuring system was improved from manual detection to automatic detection. The current research was aimed to measure the optical properties of kiwifruit tissues using the

improved automatic single integrating sphere system. Specific objectives were to: (1) establish an integrating sphere system for measuring the optical properties of biological tissue; (2) estimate the absorption coefficient μ_a and the reduced scattering coefficient μ_s' of the kiwifruit tissue using the established system and the IAD method; (3) compare the optical properties of kiwifruit tissues from three different parts (the flesh part, the seed part, and the seed-base part).

2 Materials and methods

2.1 Integrating sphere system

A schematic of the developed single integrating sphere system is shown in Fig. 1. The system was built on an optical table (Beijing Optical Century Instrument Co., Ltd., Beijing, China), including a light source, a neutral density (ND) filter, an integrating sphere with a diameter of 152 mm (model 4P-GPS-060-SF, Labsphere, North Sutton, NH, USA), a sphere port cover, a light barrier, a sample holder, an optical fiber (model QP1000-2-VIS-NIR, Ocean Optics, Dunedin, FL, USA), a spectrometer (model QE65pro, Ocean Optics, Dunedin, FL, USA), three motorized translation stages (PX245M-01A, VEXTA; TU4036-220L, IKO; Japan), a controller (STC89C516), and a computer. The integrating sphere was coated by Spectrafect[®] material, which had a reflectivity of 98%

at 632.8 nm. Two 25.4-mm-diameter ports located oppositely on the equator of the sphere were used as entrance and exit. Optical fiber was used to connect the port plug on the north pole of the sphere and the spectrometer. The light source used in this study was a He-Ne laser with an output of 632.8 nm and a beam diameter of 1 mm. The laser source was mounted on a kinematic laser holder, which could provide two axes of precision angular adjustments of the laser beam. The ND filter was used to attenuate the incident light intensity. The ND filter in the filter holder can be replaced by a series of ND filters with different optical densities (ODs) but the same size, so that the light intensity can be adjusted into an appropriate range when the light source is replaced. The OD was 1.0 in this study. The sphere port cover and the light barrier were used to cover the exit and entrance ports for different measurement purposes. The sample holder was originally designed to hold the glass cuvette or sheet sample. It has four bolts through two sides to fix the sandwiched tissue sample to make the tissue a slab. The light barrier and the sample holder were installed on a two-dimensional adjustable stage, which was combined with two motorized translation stages. The port cover was installed on another motorized translation stage. The three translation stages were controlled by the controller and the computer. The whole system was enclosed in a dark chamber consisting of optical rails and black hardboards.

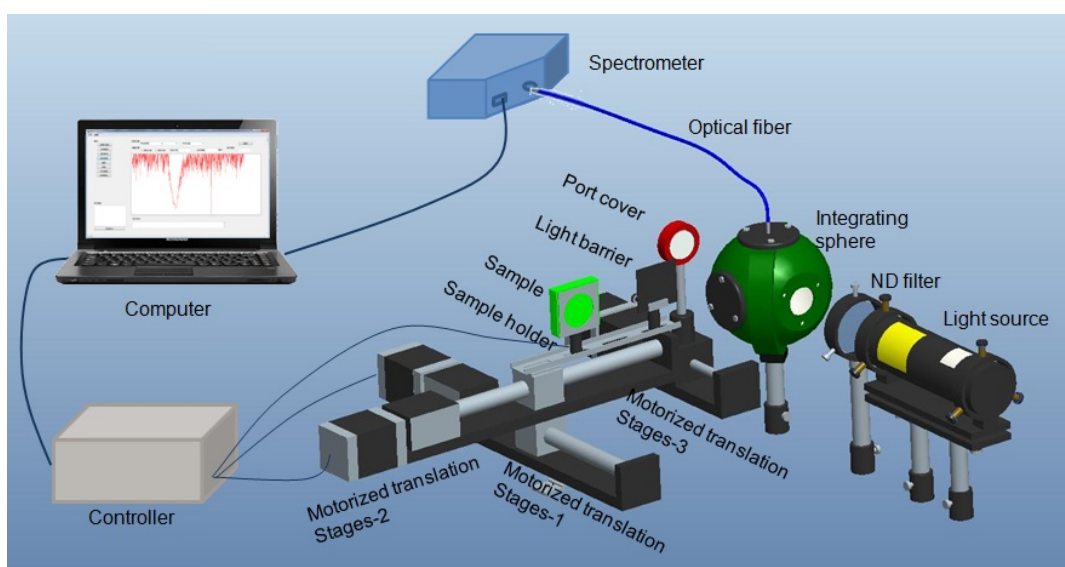


Fig. 1 Schematic of the single integrating sphere system

2.2 Reflectance and transmittance measurement

To obtain the absorption and reduced scattering coefficients based on the integrating sphere system, total transmittance (T_t), total reflectance (R_t), and the scattering anisotropy coefficient g must be known. Measurements of the total reflectance and transmittance were referenced from the setup recommended by Saeys *et al.* (2008). Before measuring the transmittance and reflectance signals, the reference and dark signals were measured. The dark background (I_{dark}) was measured by covering all ports of the integrating sphere and turning off the laser. The reference signal (I_{ref}) was measured by opening the entrance port and covering the exit port with the port cover of the sphere and turning on the laser. To measure the T_t , the sample was automatically moved to the entrance port of the sphere, while the exit port was blocked with the port cover. In this case, all light transmitted through the sample (I_t) was collected by the sphere and detected by the spectrometer through the port plug. To measure the R_t , the sample was automatically moved to the exit port of the sphere, so that all light reflected by the sample (I_r) was collected in the sphere and directed toward the spectrometer. The T_t and R_t were calculated using the detected signals of I_{dark} , I_{ref} , I_t , and I_r .

The IAD program provided by Prahl (2011) was used to calculate the optical properties for each kiwifruit tissue sample. Using the IAD program, μ_a and μ_s' can be calculated using the measured T_t and R_t signals, and g . The g value can be estimated when the collimated transmittance (T_c) was detected following the method recommended by Prahl (2011). In this study, T_c detected by the established system was too small, which influences the calculated g values significantly. Some sensitivity analysis has shown that μ_a and μ_s' estimations are not very sensitive to the value of g (Tuchin, 2007). The values of g reported were 0.55–0.75 for apple flesh (Saeys *et al.*, 2008) and 0.427–0.688 for onion flesh (Wang and Li, 2013). Our previous research also indicated that the optical properties of kiwifruit tissue were not sensitive to the value of g from 0.4 to 0.9. Therefore the g value was set to a constant of 0.7 here.

2.3 Measurement of kiwifruit tissue

“Zespri Green” kiwifruits were purchased from a local market. They were stored in a cold room at

(4 ± 1) °C before being tested. Thirty disease-free kiwifruits were manually selected. The samples were taken from the cold room 12 h prior to tests and stored at room conditions (about 15 °C, about 70% relative humidity). The kiwifruits were sliced by a slicer. When slicing, the blade was parallel to the neck-root direction, while the long axis of the kiwifruits was perpendicular to the blade. The thickness of the piece was set to 4 mm. For each kiwifruit, the first and last pieces were discarded. Then, three consecutive pieces from one end to the middle were selected as a set of tissues (including the flesh part, the seed part, and the seed-base part), as shown in Fig. 2. In total, 90 pieces of kiwifruit tissue samples were measured. The thickness of each sample tissue was measured using an electronic micrometer. On each sample, three replicates were made on the central area and the average value was used as the thickness. The refractive indices (n_D) of the tissues were measured by a refractometer (model DR-A1 plus, ATAGO, Japan).

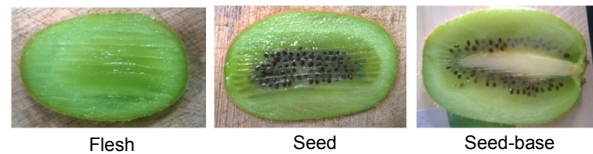


Fig. 2 Kiwifruit tissue samples of different parts

When measuring the spectral signals, the sample was sandwiched by two pieces of quartz glass ($\phi 50 \text{ mm} \times 1 \text{ mm}$). Quartz glass was used because of its good homogeneity and high transmittance at the visible range. The n_D of the quartz glass is 1.53. The T_t and R_t were measured at five positions of each sample in the same horizontal plane. Every two contiguous positions of each sample have the same distance of 2 mm.

2.4 System validation

To quantify the estimation errors of the absorption and reduced scattering coefficients, the integrating sphere system was validated using the phantoms made from Intralipid 20% (Sigma Aldrich, USA) and a Biomimic solid phantom. First, we measured the μ_a and μ_s' of the Biomimic phantom for continuous 5 d. The marked μ_a and μ_s' of the Biomimic phantom at 632.8 nm are 0.00387 mm^{-1} and 0.922 mm^{-1} , respectively. Then, the μ_a and μ_s' of Intralipid 20% solution with a different concentration were measured. The validation method was similar to that described

by Troy and Thennadil (2001) and Saeys *et al.* (2008). According to the reports, the μ_a values of kiwifruit were 0.055–0.283 mm^{-1} . The μ_s' values of kiwifruit were 0.15–0.76 mm^{-1} . Pure absorption solutions were first made by mixing small amounts of India ink with distilled water. Intralipid 20% was then pipetted into the pure absorption solutions to make emulsions diluted to the final concentrations of Intralipid 20% at 1%, 2%, 4% (v/v) and of India ink at 0.005%, 0.010%, 0.015%, 0.020% (v/v).

3 Results and discussion

3.1 Validation results of the integrating sphere system

Fig. 3 shows the μ_a and μ_s' values of the Biomimic solid phantom measured at three different time points (9:00 a.m., 2:00 p.m., 9:00 p.m.) over the continuous 5 d. Fig. 3a shows that the relative difference of the absorption coefficient is 45%, 44%, and 45%, respectively. Fig. 3b shows that the relative difference of the reduced scattering coefficient is 3.8%, 4.2%, and 4.8%, respectively, all less than 5.0%. There were no significant changes of the two parameters in 5 d detected by the system, which confirmed its stability. Fig. 4 shows the μ_a and μ_s' values of Intralipid 20% solution with different concentrations (1%, 2%, 4%) and optical paths (3, 5, 7 mm)

solution with different concentrations and optical paths. The result shows that the relative differences of the absorption and reduced scattering coefficients of Intralipid 20% solution with different concentrations are both less than 10%.

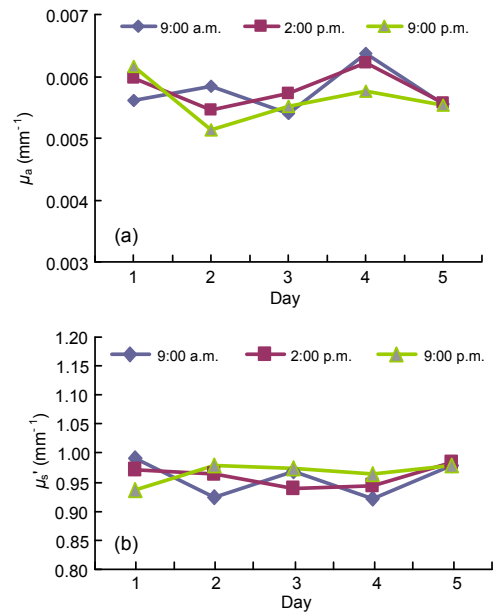


Fig. 3 μ_a (a) and μ_s' (b) values of the Biomimic solid phantom measured at three different time points (9:00 a.m., 2:00 p.m., 9:00 p.m.) over continuous 5 d

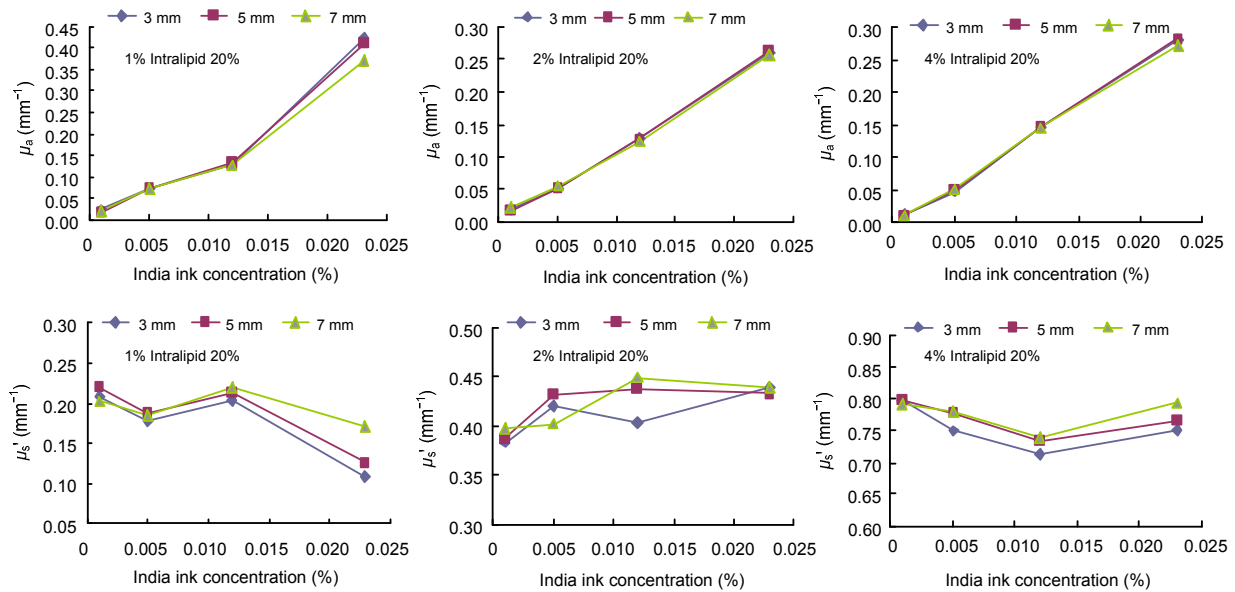


Fig. 4 μ_a and μ_s' values of Intralipid 20% solution with different concentrations (1%, 2%, 4%) and optical paths (3, 5, 7 mm)

Thus the above results indicate that the system is of good stability. The relative differences of the absorption and reduced scattering coefficients are acceptable, being in the range of $0.02\text{--}0.30\text{ mm}^{-1}$ and $0.02\text{--}0.80\text{ mm}^{-1}$, respectively, as well as the optical path in the range of $3\text{--}7\text{ mm}$. The relative difference of the absorption coefficient is large when measuring the optical properties of the Biomimic phantom. The reason may be that the Biomimic phantom is a kind of high albedo medium. The absorption coefficient of the Biomimic phantom is significantly lower than the scattering coefficient of the Biomimic phantom, 0.00387 mm^{-1} and 0.922 mm^{-1} , respectively. It leads to large errors measuring the absorption coefficient of a high albedo medium using an integrating sphere-based system. Overall, the accuracy of the system for estimating the μ_s' could meet the detecting requirement.

3.2 Reflectance and transmittance of kiwifruit tissue

Fig. 5a shows the total reflectance (R_t) values of the kiwifruit samples. The R_t values of the seed-base part were the highest among the three parts. In contrast, the R_t values of the seed part were the smallest. The deviations of the R_t values among different positions on one piece and among different pieces of three parts were small. Fig. 5b shows the total transmittance (T_t) values of the samples. The trend shown in Fig. 5b was different from that in Fig. 5a. For the T_t , the deviations among different positions of the seed part were the largest. The deviations among different pieces of the three parts were similar.

The main reason for this situation was that the kiwifruit tissue was a heterogeneous medium, especially the seed part. As Fig. 2 shows, seeds were randomly distributed at the center area of the seed part. When the translation stages moved for the total transmittance and the total reflectance measurements at different positions of each sample, whether the light beam irradiated the seeds or not made a significant difference to the results. The IAD method can only be accurate on a spatially homogenous medium since it assumes that layers to be doubled have identical optical properties. The seed part was so heterogeneous that the optical properties in the light path were significantly different. Thus, the measurement error of IAD can be quite significant. The results on seed part may therefore be unreliable. Fig. 2 also shows that the center area (the white area) of the seed-base part was the most homogeneous among the three parts. That explains why the deviations of both the R_t and T_t values among different positions of the seed-base part were smaller than those of the other two parts. The detected spectral signals concern the optical properties of the tissue in a very small area that the laser beam irradiated. Therefore, it is necessary to acquire spectral signals from different positions, especially for heterogeneous media.

3.3 Absorption and reduced scattering coefficients of kiwifruit tissue

The average thickness and refractive index of samples of the flesh part, seed part, and seed-base part were 4.35 , 4.43 , 4.24 mm and 1.338 , 1.335 , and 1.342 ,

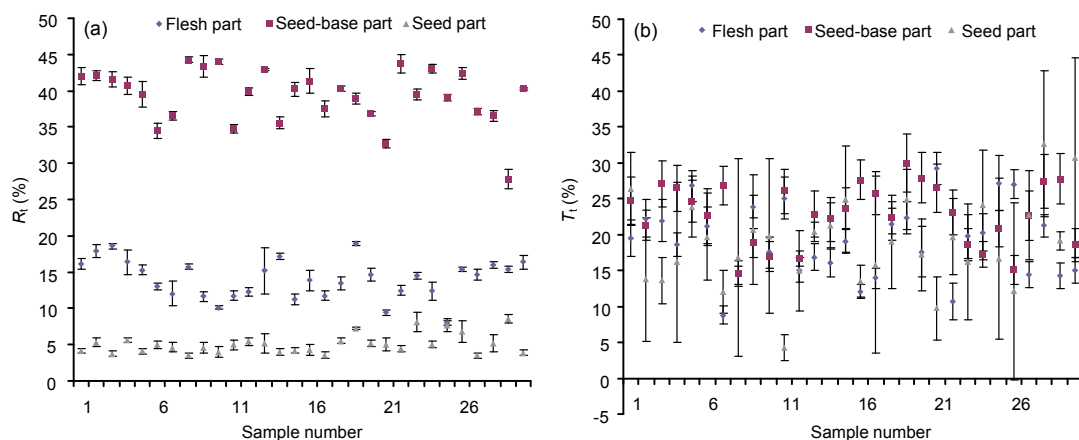


Fig. 5 Total reflectance R_t (a) and total transmittance T_t (b) of each piece of kiwifruit tissues (flesh part, seed part, and seed-base part) at 632.8 nm

Data are expressed as mean \pm standard deviation (SD) at five positions of each sample (total 30 samples)

respectively. Fig. 6 shows the mean and standard deviation values of μ_a and μ_s' of the tissues of different parts estimated by the IAD program. According to the mean values of the μ_a , the light absorption of tissue in the seed part was about 10 times higher than that of tissue in the seed-base part. The μ_a of the flesh part was between those of the other two parts. The μ_s' of the seed-base part was about 8 times higher that of the seed part. The μ_s' of the flesh part was between those of the other two parts, which was similar to the situation of μ_a . Table 1 shows results of analysis of variance (ANOVA) for the optical properties of different parts of kiwifruits. The results indicated that the μ_a and μ_s' of the three parts were significantly different, with the P -values being less than 0.01.

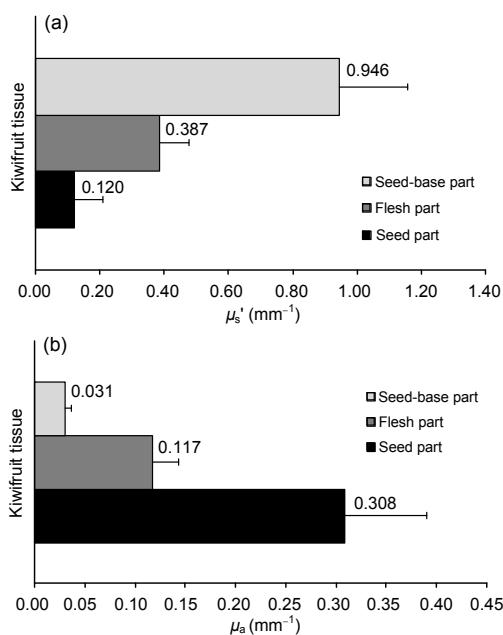


Fig. 6 μ_s' (a) and μ_a (b) of kiwifruit tissues of the flesh part, seed part, and seed-base part at 632.8 nm
Data are expressed as mean \pm SD (total 30 samples)

The absorption differences of the three parts were due to their pigments. The dark color of the seeds in the seed part and the white color of the tissue in the seed-base part were the main reason for the highest and lowest μ_a values, respectively. The significant differences of the μ_s' values of the three parts might be caused by the different tissue microstructures of the three parts. For tissues of the flesh part and the seed-based part, the μ_s' values were much larger than the μ_a values, which was consistent with the statement that fruits are high scattering biological media. The exception of tissue of the seed part may be due to the randomly distributed seeds in this part.

Generally, the μ_a values of kiwifruit tissue detected by the established integrating sphere system and the IAD method were comparable to those reported in other research (Zerbini *et al.*, 2002; Qin and Lu, 2008). The μ_a values of kiwifruit reported by Zerbini *et al.* (2002) were 0.005–0.450 mm⁻¹ in the range of 650–1000 nm based on the TRS technique. In the study of Qin and Lu (2008), the μ_a values of kiwifruit were 0.02–0.10 mm⁻¹ in the range of 500–1000 nm based on the HISR method. However, the μ_s' values of kiwifruit tissues detected in this study were much smaller than those detected by Zerbini *et al.* (2002) (1.0–1.6 mm⁻¹ in the range of 650–1000 nm) and Qin and Lu (2008) (0.7–0.8 mm⁻¹ in the range of 500–1000 nm). The differences of the μ_a and μ_s' values detected in these studies may partly be due to the different varieties of the kiwifruit samples, the different methods used as well as the different wavelength ranges.

4 Conclusions

The optical properties of kiwifruits at the wavelength of 632.8 nm were investigated. The mean

Table 1 Results of ANOVA for the optical properties of kiwifruit tissues at 632.8 nm

Optical property	Source	SS	df	MS	F	P-value	F crit
μ_a	Between group	1.163050	2	0.581525	154.6199	2.21×10^{-28}	3.109311
	In group	0.304641	81	0.003761			
	Total	1.467691	83				
μ_s'	Between group	5.631531	2	2.815765	171.8217	7.22×10^{-30}	3.103839
	In group	1.327405	81	0.016388			
	Total	6.958936	83				

SS: sum of squares of deviations; df: degrees of freedom; MS: mean square; F: F-statistic; F crit: F critical value

values of μ_a and μ_s' of tissues in different parts of kiwifruit were 0.031–0.308 mm^{-1} and 0.120–0.946 mm^{-1} at 632.8 nm, respectively. At this wavelength, the μ_s' values were much larger than the μ_a values of tissue in the flesh part and the seed-based part. In contrast, μ_a was larger than μ_s' for tissue in the seed part. The results revealed the significant differences of optical properties of kiwifruit tissue in different parts. It can be confirmed that studying the optical properties of fruit tissue is very important for understanding light interaction with different kinds of tissue. The measured absorption and scattering characteristics of fruit tissue may help to better design optical systems for quality evaluation. Based on this study, further investigation will be extended to a broader spectral region and different kinds of fruits.

Compliance with ethics guidelines

Zhen-huan FANG, Xia-ping FU, and Xue-ming HE declare that they have no conflict of interest.

This article does not contain any studies with human or animal subjects performed by any of the authors.

References

- Birth, G.S., 1978. The light scattering properties of foods. *J. Food Sci.*, **43**(3):916-925.
- Cen, H., Lu, R., Mendoza, F.A., et al., 2012. Assessing multiple quality attributes of peaches using optical absorption and scattering properties. *Trans. ASABE*, **55**(2):647-657. <http://dx.doi.org/10.13031/2013.41366>
- Chen, J., Wang, X.Z., 2001. A new approach to near-infrared spectral data analysis using independent component analysis. *J. Chem. Inform. Comput. Sci.*, **41**(4):992-1001. <http://dx.doi.org/10.1021/ci0004053>
- Cheong, W.F., Prahl, S.A., Welch, A.J., 1990. A review of the optical properties of biological tissues. *IEEE J. Quantum Electron.*, **26**(12):2166-2185. <http://dx.doi.org/10.1109/3.64354>
- Cubeddu, R., D'Andrea, C., Pifferi, A., et al., 2001a. Nondestructive quantification of chemical and physical properties of fruits by time-resolved reflectance spectroscopy in the wavelength range 650–1000 nm. *Appl. Opt.*, **40**(4):538-543. <http://dx.doi.org/10.1364/AO.40.000538>
- Cubeddu, R., D'Andrea, C., Pifferi, A., et al., 2001b. Time-resolved reflectance spectroscopy applied to the nondestructive monitoring of the internal optical properties in apples. *Appl. Spectrosc.*, **55**(10):1368-1374. <http://dx.doi.org/10.1366/0003702011953496>
- Fang, Z., Fu, X., 2014. Measurement of optical properties of kiwifruit tissues using a single integrating sphere based system. 2014 ASABE and CSBE/SCGAB Annual International Meeting. July 13–16, 2014, Montreal, Quebec, Canada, **5**:3607-3615.
- Kim, A., Wilson, B.C., 2011. Measurement of ex vivo and in vivo tissue optical properties: methods and theories. In: Welch, A.J., van Gemert, M.J.C. (Eds.), *Optical-Thermal Response of Laser-Irradiated Tissue*. Springer Netherlands, p.267-319. http://dx.doi.org/10.1007/978-90-481-8831-4_8
- Lu, R., Cen, H., Huang, M., et al., 2010. Spectral absorption and scattering properties of normal and bruised apple tissue. *Trans. ASABE*, **53**(1):263-269. <http://dx.doi.org/10.13031/2013.29491>
- Pickering, J.W., Prahl, S.A., van Wieringen, N., et al., 1993. Double-integrating-sphere system for measuring the optical properties of tissue. *Appl. Opt.*, **32**(4):399-410. <http://dx.doi.org/10.1364/AO.32.000399>
- Prahl, S., 2011. Everything I think you should know about Inverse Adding-Doubling. Oregon Medical Laser Center, Manual of the Inverse Adding-Doubling Program. Available from <http://omlc.ogi.edu/software/iad/>.
- Prahl, S.A., van Gemert, M.J.C., Welch, A.J., 1993. Determining the optical properties of turbid media by using the adding-doubling method. *Appl. Opt.*, **32**(4):559-568. <http://dx.doi.org/10.1364/AO.32.000559>
- Qin, J., Lu, R., 2008. Measurement of the optical properties of fruits and vegetables using spatially resolved hyperspectral diffuse reflectance imaging technique. *Postharvest Biol. Technol.*, **49**(3):355-365. <http://dx.doi.org/10.1016/j.postharvbio.2008.03.010>
- Qin, J., Lu, R., 2009. Monte Carlo simulation for quantification of light transport features in apples. *Comput. Electron. Agric.*, **68**(1):44-51. <http://dx.doi.org/10.1016/j.compag.2009.04.002>
- Rizzolo, A., Vanoli, M., Spinelli, L., et al., 2010. Sensory characteristics, quality and optical properties measured by time-resolved reflectance spectroscopy in stored apples. *Postharvest Biol. Technol.*, **58**(1):1-12. <http://dx.doi.org/10.1016/j.postharvbio.2010.05.003>
- Saeyns, W., Velazco-Roa, M.A., Thennadil, S.N., et al., 2008. Optical properties of apple skin and flesh in the wavelength range from 350 to 2200 nm. *Appl. Opt.*, **47**(7):908-919. <http://dx.doi.org/10.1364/AO.47.000908>
- Troy, T.L., Thennadil, S.N., 2001. Optical properties of human skin in the near infrared wavelength range of 1000 to 2200 nm. *J. Biomed. Opt.*, **6**(2):167-176. <http://dx.doi.org/10.1117/1.1344191>
- Tuchin, V., 2007. *Tissue Optics: Light Scattering Methods and Instruments for Medical Diagnosis*, 2nd Ed. SPIE Press, Bellingham, Washington, p.143-208. <http://dx.doi.org/10.1117/3.684093>
- Vanoli, M., Zerbini, P.E., Spinelli, L., et al., 2009. Polyuronide content and correlation to optical properties measured by time-resolved reflectance spectroscopy in 'Jonagored' apples stored in normal and controlled atmosphere. *Food Chem.*, **115**(4):1450-1457. <http://dx.doi.org/10.1016/j.foodchem.2009.01.081>
- Vanoli, M., Rizzolo, A., Grassi, M., et al., 2014. Studies on classification models to discriminate 'Braeburn' apples affected by internal browning using the optical properties measured by time-resolved reflectance spectroscopy.

Postharvest Biol. Technol., **91**:112-121.

<http://dx.doi.org/10.1016/j.postharvbio.2014.01.002>

Wang, W., Li, C., 2012. The optical properties of onion dry skin and flesh at the wavelength 632.8 nm. *In: Proc. SPIE 8369, Sensing for Agriculture and Food Quality and Safety IV*, 83690G. Baltimore, Maryland, USA.

<http://dx.doi.org/10.1117/12.919855>

Wang, W., Li, C., 2013. Measurement of the light absorption and scattering properties of onion skin and flesh at 633 nm. *Postharvest Biol. Technol.*, **86**:494-501.

<http://dx.doi.org/10.1016/j.postharvbio.2013.07.032>

Zerbini, P.E., Grassi, M., Cubeddu, R., et al., 2002. Nondestructive detection of brown heart in pears by time-resolved reflectance spectroscopy. *Postharvest Biol. Technol.*, **25**(1):87-97.

中文概要

题目: 基于单积分球系统的猕猴桃组织吸收和散射特性

目的: 开展水果组织的光传输特性检测分析, 以猕猴桃组织为例探讨其在 632.8 nm 波长的光传输特性。

创新点: 开发基于单积分球的水果组织光传输特性自动检测系统, 验证其可靠性并应用于水果组织的分析, 并获得猕猴桃组织不同部位在 632.8 nm 的吸收和散射系数。

方法: 利用所搭建的单积分球系统, 获取三个不同部位(果肉、种子和种子基座)组织的全反射和全透射信息, 测量各个组织切片的厚度及折射率。运用逆倍增算法计算得到各组织样本的吸收系数 μ_a 和约化散射系数 μ_s' , 并根据计算所得结果对猕猴桃不同组织的光传输特性进行比较分析。

结论: 本实验结果测得猕猴桃不同部位组织的吸收系数和散射系数分别为 0.031~0.308 mm^{-1} 和 0.120~0.946 mm^{-1} , 并显示猕猴桃不同部位组织的吸收和散射特性具有显著差异。种子部位受随机分散的种子的影响较大, 组织较均匀的果肉和种子基座部位结果证实散射系数大于吸收系数, 符合生物组织高散射介质特性。这些结果说明了定量测定组织的光传输特性参数对深入研究光与水果组织相互作用的重要性。

关键词: 光学特性; 积分球; 逆倍增算法; 猕猴桃